ORIGINAL ARTICLE

Effect of thermal spray processes on microstructures and properties of Ni-20%Cr coatings

Nuchjira Dejang[1], Pittaya Kuntasudjai[2] and Sukanda Jiansirisomboon[3]

Abstract

Dejang, N., Kuntasudjai, P. and Jiansirisomboon, S.
Effect of thermal spray processes on microstructures and properties of Ni-20%Cr coatings
Songklanakarin J. Sci. Technol., 2006, 28(3) : 677-686

Ni-20%Cr coatings were produced using different thermal spray techniques, which were spray and fuse, flame spray and arc spray. The Ni-20%Cr powder was sprayed onto a mild steel substrate using the spray and fuse and the flame spray systems, while the Ni-20%Cr wire was sprayed using the arc spray system. SEM microstructures of the coatings suggested the spraying conditions used were able to produce dense microstructures. However, the microstructure of the arc sprayed coatings showed fine lamellar characteristics compared to the coatings prepared by the spray and fuse and the flame spray techniques. Chemical elements and oxide were quantified by EDS-SEM technique. Differences in microstructure and coating characteristics such as content of porosity and oxide due to different processing techniques significantly affected the coating properties such as adhesion strength, hardness and wear rate.

Key words : thermal spray, coating, Ni-20%Cr, microstructure, adhesion strength, hardness, wear

[1]M.Sc.(Physics), [2]B.Sc.(Materials Science), [3]D.Phil.(Materials Science), Department of Physics, Faculty of Science, Chiang Mai University, Muang, Chiang Mai 50200, Thailand.
Corresponding e-mail: sukanda@chiangmai.ac.th
Received, 26 September 2005 Accepted, 22 November 2005

บทคัดย่อ

นุชจิรา ดีแจ้ง[1] พิทยา กันทะสุดใจ[1] และ สุกานดา เจียรศิริสมบูรณ์[1]

อิทธิพลของกระบวนการพ่นด้วยความร้อนที่มีต่อโครงสร้างจุลภาค และสมบัติของผิวเคลือบนิเกิล-20%โครเมียม

ว. สงขลานครินทร์ วทท. 2549 28(3) : 677-686

ผิวเคลือบนิเกิล-20%โครเมียมได้ถูกเตรียมขึ้นโดยเทคนิคการพ่นเคลือบด้วยความร้อนต่างชนิดกัน ได้แก่ การพ่นแบบพ่นและหลอม การพ่นแบบเปลวไฟ และการพ่นแบบอาร์ค โดยผงนิเกิล-20%โครเมียมจะถูกพ่นลงบนผิวรองรับที่เป็นเหล็กอ่อนโดยระบบพ่นแบบพ่นและหลอม และแบบเปลวไฟ ในขณะที่ลวดนิเกิล-20%โครเมียมจะถูกพ่นด้วยระบบพ่นแบบอาร์ค โครงสร้างจุลภาคจากกล้องจุลทรรศน์อิเล็กตรอนแบบส่องกราดของผิวเคลือบชี้ให้เห็นว่าเงื่อนไขการพ่นที่ใช้นั้น สามารถผลิตโครงสร้างจุลภาคที่หนาแน่นได้ อย่างไรก็ตาม โครงสร้างจุลภาคของผิวเคลือบที่ได้จากการพ่นแบบอาร์คแสดงลักษณะเฉพาะของชั้นผิวเคลือบที่ละเอียดมาก เมื่อเปรียบเทียบกับผิวเคลือบที่เตรียมจากเทคนิคพ่นและหลอม และพ่นแบบเปลวไฟ ปริมาณธาตุทางเคมีและออกไซด์ถูกวิเคราะห์ด้วยเทคนิคกระจายพลังงานของรังสีเอ็กซ์ ความแตกต่างของโครงสร้างจุลภาคและลักษณะเฉพาะของผิวเคลือบ เช่น ปริมาณรูพรุน และปริมาณออกไซด์ เนื่องจากเทคนิคการพ่นเคลือบด้วยความร้อนต่างชนิดกันนั้น จะส่งผลต่อสมบัติของผิวเคลือบ เช่น ความแข็งแรงการยึดเกาะ ความแข็ง และอัตราการสึกหรอ เป็นอย่างยิ่ง

ภาควิชาฟิสิกส์ คณะวิทยาศาสตร์ มหาวิทยาลัยเชียงใหม่ ตำบลสุเทพ อำเภอเมือง จังหวัดเชียงใหม่ 50200

Thermal spray is an established industrial method for the surfacing and resurfacing of many engineering parts. A major advantage of thermal spray processes is the wide variety of materials that can be used to produce coatings (Tucker, 1994). Virtually any materials that melt without decomposing can be used. A second major advantage is the ability to apply coating to substrate without significant heat input. Thus, no changing of the properties of the part and no excessive thermal distortion occurred. A third major advantage is the ability to strip off and restore worn and damaged coatings without changing part properties and dimensions. Thermal spray, therefore, offers typically lower cost, improved engineering performance and increased component life. New designs in thermal spray equipments and materials have resulted in attractive coating solutions in the aerospace, industrial gas turbine, petrochemical and gas and automotive industries, etc.

Coating build-up process can occur rapidly by four processes which are melting, accelerating droplets to speeds in the range of 50 to >1000 ms^{-1}, impacting and solidifying onto a substrate. Microstructure of a thermal-sprayed coating in general is lamellar in nature formed by flattened splat of individual particles. There are defects such as microcracks and different kinds of pore, which affect and are closely associated with the properties of the coatings and their applications (Pawlowski, 1995).

Thermal spray can be divided into many techniques depending on energy sources used to melt the starting materials. Five basic thermal spray processes are available, i.e. flame spray (FS), detonation (D-Gun) and high velocity oxygen fuel (HVOF) are three of the basic processes associated with combustion. Plasma spray (PS) and wire arc spray (AS) are two other processes that utilize electrical energy to help melt consumable materials (Thorpe, 1993; Pawlowski, 1995). Selection of the appropriate thermal spray process is typically determined by desired coating material, coating performance requirement, economics, part size and portability. In this study, only flame spray and arc spray processes were selected to produce Ni-20%Cr coatings. However, the flame spray process

included 2 spray systems which were the flame spray and the spray and fuse. The latter system is much cheaper due to the less complicated gun design with uncontrollable powder feed rate. Details of the flame and the spray and fuse guns are given in the section of materials and methods. In the flame spray process, the powder is aspirated into the oxygen-fuel flame, melts and carried by flame and air jets to impact onto the substrate as schematically shown in Figure 1. Particle speed is relatively low, and bond strength is also generally low compared to other high velocity processes (Thorpe, 1993). In the arc spray process or sometimes called the wire arc spray, two consumable wire electrodes are connected to a high direct current (dc) power source, fed into the gun and meet, establishing an arc between them that melts the tips of the wires. The melted material is then atomized and propelled toward the substrate by a stream of air as schematically shown in Figure 2. The process is energy efficient because all of input energy is used to melt the material (Thorpe, 1993). Table 1 compares important process characteristics associated with the flame spray and arc spray processes.

Ni-based metallic alloy such as Ni-Cr are widely used in applications where wear resistance combined with oxidation or hot corrosion resistance is required. This material is currently used in the chemical industry, petroleum industry, glass mould industry, and for hot working punches and fan blades factories, etc. Recent works reporting on Ni-Cr coatings are mostly related to HVOF technique (Sundararajan *et al*., 2003; Sundararajan *et al*., 2005; Sidhu *et al*., 2005). The objective of this work was to produce the Ni-20%Cr coatings using three thermal spray processes, namely, spray and fuse, flame spray and arc spray. Microstructure and chemical composition of as-sprayed coatings were characterized. The coating properties such as adhesion strength, hardness and wear rate are evaluated. Relations between microstructure, chemistry and properties of the coating are reported and discussed.

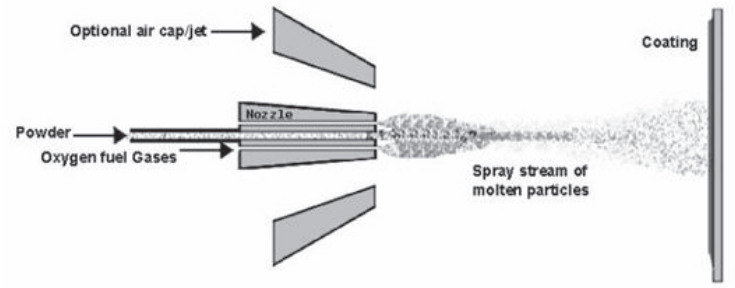

Figure 1. Schematic diagram of flame spray process.

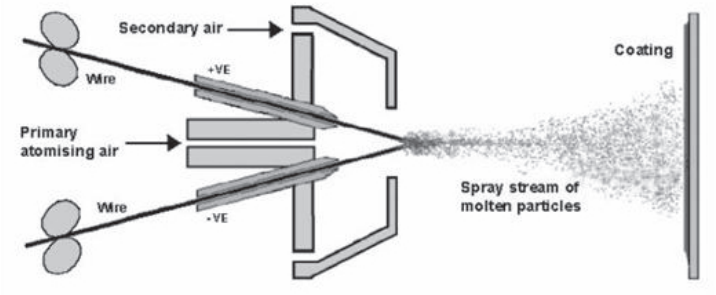

Figure 2. Schematic diagram of arc spray process.

Table 1. Comparison of thermal spray processes (edited after Thorpe, 1993)

Parameters	Flame spray	Arc spay
Gas flow (m^3h^{-1})	11	71
Flame temperature (ºC)	2200	5500
Particle impact velocity (ms^{-1})	30	240
Relative adhesive strength *	3	6
Cohesive strength	Low	High
Oxide content (%)	6	0.5-3
Relative process cost *	3	1
Maximum spray rate (kgh^{-1})	7	16
Power (kW)	25-75	4-6
Energy required to melt ($kWkg^{-1}$)	11-22	0.2-0.4

*** 1 (low) to 10 (high)**

Materials and Methods

Materials

Starting material used in this research was nickel with 20 wt% chromium alloy (Ni-20%Cr) in two different forms, namely, powder (Hoganas, Sweden) and wire (1.6 mm in diameter, Flame Spray Technologies, Netherlands). Both morphology and chemical composition of the starting materials were analyzed using a scanning electron microscope (SEM) and energy dispersive spectroscopy (EDS-SEM, JEOS JSM-5910, Japan), respectively. At least 5 areas or points were selected for EDS-SEM analysis to minimize any experimental errors that could occur.

Coating Preparation

Commercial as-received Ni-20%Cr powder and wire were sprayed onto grit-blasted mild steel substrates with a diameter of 25 mm and 5 mm thick. Thermal spraying was prepared using a spray and fuse gun (SF, Karta-201, India), flame spray gun (FS, MEC powderjet-86, India) and arc spray gun (AS, Tafa Arcjet 9000, India) as shown in Figure 3. The conditions used for spraying were recommended by the guns' manufacturers as listed in Table 2. The spray principles of SF and FS processes were similar in terms of thermal source, i.e. a combustion flame. However, a powder feed system of the two systems were significantly different. Powder flowed by a gravimetric force in the SF system while it used powder carrier gas (N_2) with adjustable flow rate of powder in the FS system. Apart from this, powder in the SF system met the flame and was heated right in front of the SF gun, while powder flowing through the FS gun could absorb more heat for a longer period because the powder flowed through the gun nozzle along with the flame. Therefore, the powder could be melted more easily in the FS system compared to the SF system. In the AS system, an electric arc was used as the heat source. Two Ni-20%Cr wires from two external rolls were continuously fed at a controlled speed through the AS gun. Coatings of at least 300 μm thickness well-adhered onto substrates were finally achieved, and were further investigated in detail.

Material Characterization

The as-sprayed coatings were cross-sectioned using a cutting machine (Struers Labotom-3, UK) and mounted in resin (Struers Lonbotom-1, UK). The samples were then ground using SiC papers with the grit size 100, 400, 600, 1000, 1200 and finally polished with 1 μm alumina. Percentage of porosity was calculated from optical microstructure of these samples by an image analysis method (Olympus micro image version 4.0 program, USA). At least 5 areas were carefully selected to minimize material pull-out during

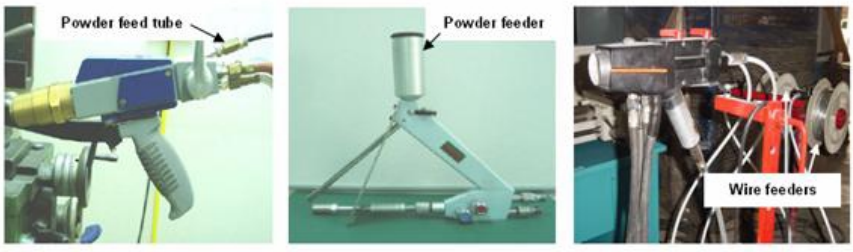

Figure 3. Thermal spray guns (a) spray and fuse, (b) flame spray and (c) arc spray.

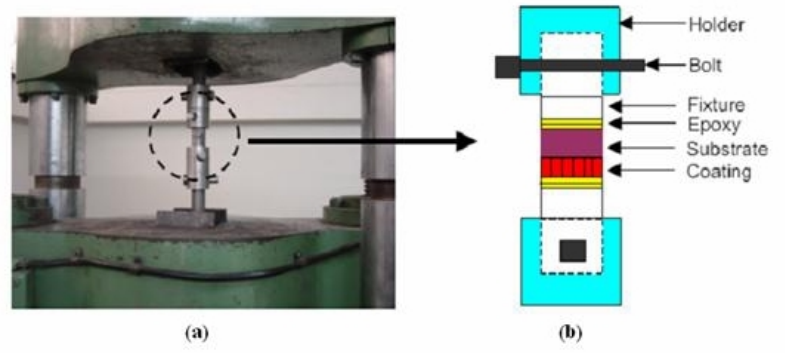

Figure 4. Experimental set-up for adhesion strength test (a) an adhesion test jig and (b) schematic diagram of the jig.

Table 2. Spray parameters for spray and fuse, flame spray and arc spray systems

Parameters	SF	FS	AS
Fuel gasses:			
Acetylene (bar)/flow rate (m^3min^{-1})	0.7/0.0	1.0/0.026	-
Oxygen (bar)/flow rate (m^3min^{-1})	3.0/0.0	2.2/0.021	-
Powder carrier gas:			
Nitrogen (bar)/flow rate (m^3min^{-1})	-	7.0/0.035	-
Powder flow rate ($gmin^{-1}$)	60	75	-
Spray distance (mm)	180	205	205
Current (A)	-	-	150
Voltage (V)	-	-	30
Air pressure (bar)	-	-	3.5

mechanical polishing. The coating morphology and chemical composition were revealed by SEM (JEOS JSM-5910, Japan) and energy dispersive spectroscopy (EDS-SEM, JEOS JSM-5910, Japan). The EDS-SEM results were then compared with the chemical elements detected in the starting materials. Adhesion strength measurement following the ASTM C633-79 standard was also employed. The coatings were firstly attached to a sample holder or jig as shown in Figure 4 by Plasmatex klebbi glue (Plasma-Technik AG, Switzerland), left to dry in an oven before subjected to a universal tester (Pa 16127 Blanwin, Germany) for the determination of a maximum load needed

for coating-substrate separation. Hardness measurement was done by Vickers hardness tester (Galileo Microscan OD, UK). The Vickers micro-indenter was pressed on the polished cross-sections and held for 15 s using a 100 g load. Disk shape coatings attached to substrate were also subjected to Pin-on-Disk machine (ISC-200 Tribometer, USA) following the ASTM G99-90a standard. Before testing, the samples were polished for flat surfaces. Wear measurement was performed using a tungsten carbide (WC) ball at 150 g load with a measured distance of 75 m. Weight loss due to wear was then used for the calculation of wear rate.

Results and Discussion

Before a production of coatings, Ni-20%Cr powder and wire were morphologically analyzed by SEM as shown in Figure 5. The powder had a spherical shape and narrow particle size distribution with a mean particle size of 50 μm (Figure 5(a)). This typical shape of powder was achieved by an atomization method as indicated by the powder's manufacturer. As-received Ni-20%Cr wire was 1.6 mm in diameter. Cross-sectional wire was homogeneous as shown in Figure 5(b). Content of elements presented in the starting materials was analyzed by EDS-SEM technique and the results are given in Table 3. It can be seen that both powder and wire consisted of only Ni and Cr with weight ratio about 80:20.

Microstructures of different coatings are shown in Figure 6. Dense coatings were successfully achieved with all spray conditions given in Table 2. Lamellar structure of the powder spray coatings, i.e. SF (Figure 6(a)) and FS (Figure 6(b)), was rougher than that of the wire AS coating (Figure 6(c)). Splat thickness was maximized in SF and reduced in FS and AS coatings, respectively. The finest in the AS coating was only a few microns thick. The splat characteristic depended directly on a degree of powder melting during spraying. In general, every individual particle could not be completely melted because the flight time and cooling rate of molten droplets were extremely fast, typically $>10^6$ Ks^{-1} for metals, which limited the ability of particle melting process (Smith and Knigth, 1995; Herman and Sampath, 1996). The droplets could impact in many forms depending on the size of the original particle. For example, a small particle could easily adsorb heat which then caused a completely melted splat, a medium-size particle could be partially melted and a large particle could not be melted. From this explanation, it suggests that the SF and FS coatings comprised different degrees of molten splats as can be seen in Figure 6(a) and 6(b). However, the coating build-up process was relatively different in the AS system. The thin splat of AS coating could be easily achieved due to the compressed air jet used at the melting zone, which helped break up the melted droplet into very fine atomization. These fine droplets then formed thin splats upon impact and solidified onto the substrate. Apart from splats, all coatings also comprised of porosity, interlamelar porosity, oxide and unmelted particles.

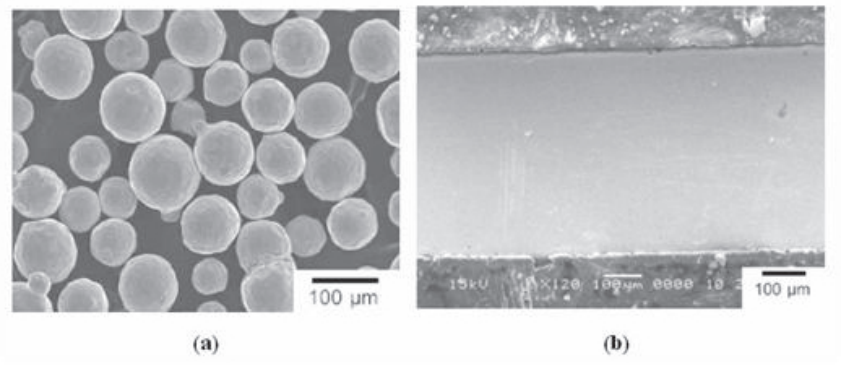

Figure 5. SEM micrographs of as-received Ni-20%Cr (a) powder and (b) wire.

Table 3. Percentage by weight of element detected by EDS-SEM analysis

Elements	% by Weight				
	Powder	SF coating	FS coating	Wire	AS coating
Ni	80.19	75.50	73.42	79.99	72.00
Cr	19.81	22.10	18.83	20.01	19.73
O	-	2.40	7.75	-	8.27
Total	100.00	100.00	100.00	100.00	100.00

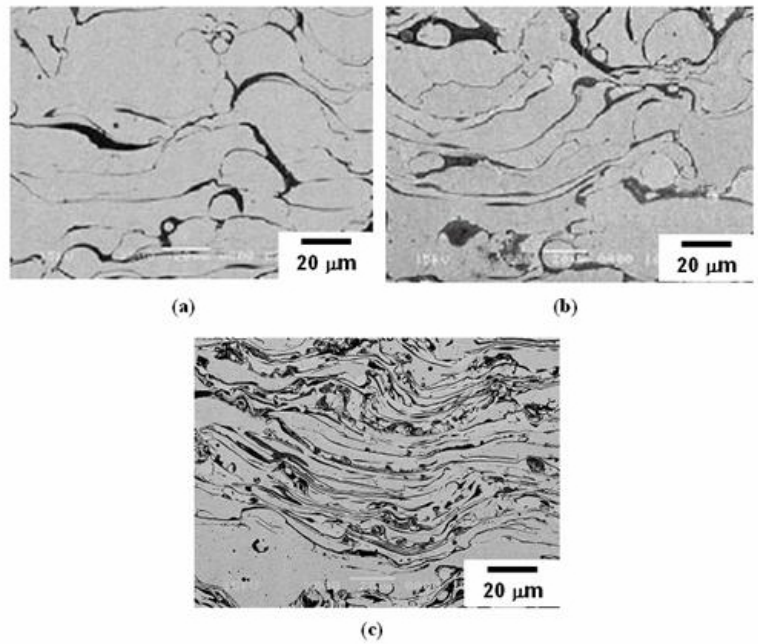

Figure 6. SEM micrographs of cross-sectional (a) spray and fuse, (b) flame spray and (c) arc spray Ni-20%Cr coatings.

Values of porosity and oxide in these coatings will be given and discussed later in detail. It can be noticed that the interlamellar porosity tended to become larger in the coating contained large splat size, i.e. SF and FS coatings, and vice versa for the AS coating. This type of porosity should be minimized by adjusting spray parameters. Otherwise, they will cause further degradation and finally failure of the coatings.

Chemical composition of the coatings was analyzed by EDS-SEM technique as shown in Table 3. All coatings comprised not only Ni and Cr elements as detected in the powder and wire, but also O element. Percentage of oxygen increased in the SF, FS and AS coatings, respectively. This was a consequence of an oxidation process occurring during spraying, which formed oxide compounds such as NiO and/or Cr_2O_3. This result corresponded to the microstructure in Figure 6 which showed a grey phase particularly incorporated at the interlamellar splats. This phase was analyzed by a point analysis of EDS-SEM technique and found to be an oxide-rich phase.

Coating characteristics in terms of percentages of porosity and oxide are summarized in Table 4. The AS coating contained minimum porosity of 8.85% compared to the SF and FS coatings. This could be explained by a good melt-

Table 4. Coating characteristics, mechanical and wear properties

Characteristics and Properties	SF	FS	AS
Content of porosity (%)	11.84±1.8	10.97±0.2	8.85±1.0
Content of oxide (%)	7.50±0.8	14.64±2.7	15.01±1.8
Adhesion strength (MPa)	16.72±1.5	19.08±2.2	25.24±2.6
Vickers hardness (HV100g)	225±11	244±19	295±28
Wear rate (mm^3m^{-1}) $\times 10^{-4}$	5.66±0.6	2.51±0.8	0.83±0.4

ing of the starting materials as already discussed. The oxide content was minimum (7.50%) in the SF coating whereas the values were very similar in FS (14.64%) and AS (15.01%) coatings. It is widely known that the amount of oxide depended significantly on the spray processes. In this study, the SF process could not properly melt the powder due to the particle flowing with gravimetric force which then speeded up an in-flight process. Therefore, the SF particle had less time to react with oxygen in the spraying atmosphere. On the other hand, the particles in the FS process were exposed in oxidizing condition at high temperature for a longer time because of the controllable particle gas (N_2) flow rate used. Fine atomization in the AS process also increased the particle surface area, which certainly increased the oxidation reaction.

Table 4 also shows adhesion strength, hardness and wear properties of all coatings. These characteristics were strongly affected by the porosity, oxide and microstructure of the coatings. Maximum adhesion strength increased in the SF, FS and AS coatings, respectively. The densest microstructure with lowest content of porosity and the adhesion characteristic between the coating and substrate were responsible for the maximum adhesion strength in the AS coating. It can be clearly seen from the AS microstructure (Figure 6(c)) that most of splats homogeneously attached to each other due to less obstructions such as unmelted particles and large porosity as commonly found in the SF and FS coatings. This kind of microstructure also increased cohesion strength within the coatings. Moreover, the use of pressurized air jet during spraying in the AS process gave well-melted splats which flowed at high speed and well-attached upon impact onto the substrate. This significantly increased the adhesion strength in the AS coating (25.24 MPa) over those values belonging to the SF (16.72 MPa) and FS (19.08 MPa) coatings. Investigation of hardness by Vickers micro-indentation indicated that the values increased in the SF, FS, and AS coatings as listed in Table 4. The main reason for the maximum hardness in the AS coating was not only the dense splat microstructure with low porosity, but also the highest content of oxide. In general, the oxide compounds were harder than metals and alloys. Therefore, the oxide phases presented in the coatings helped to increase hardness in the Ni-Cr alloy. Abrasive wear characteristics of each polished coating were investigated using a Pin-on-Disk method. The wear mechanism occurs when asperities of a rough, hard surface (WC ball) slide on a softer surface and damage the interface by plastic deformation or fracture as shown by the wear scars in Figure 7. These wear scars also suggested that the severity of wear damage was different in each coating. These wear scars exhibited 2 distinct features: grooves along the direction of abrasive flow and holes which appeared as dark regions. These holes resulted from either porosity originally present in the coatings or fracture occurring during the abrasion process. According to the wear scars shown in Figure 7, the SF coating had a higher content of holes than the FS and AS coatings. The more holes present in the coating, the greater the wear rate because of the large area of opened surfaces to wear. It is also clear that the track widths were maximum in the SF coating and minimum in the AS coating. This

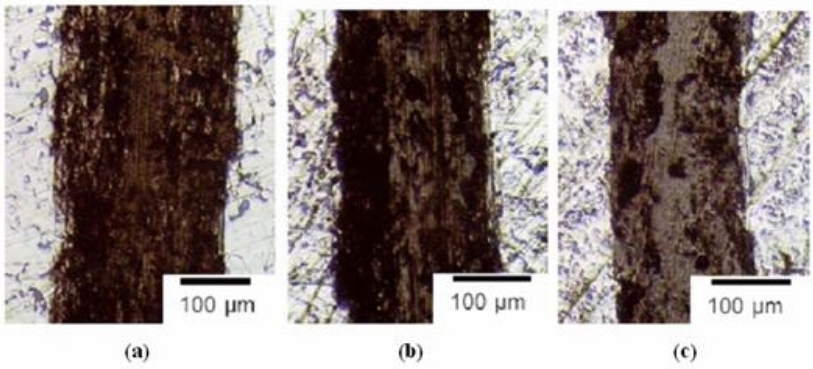

Figure 7. Wear tracks of (a) spray and fuse, (b) flame spray and (c) arc spray Ni-20%Cr coatings.

can be directly explained by the coating characteristics: content of porosity and oxide. As mentioned earlier, the high oxide and low porosity contents gave rise to the hard coating, which then increased the resistance to wear damage. According to hardness-wear relationship (Bhushan and Gupta, 1997); the harder the coating, the less wear rate can be achieved. The wear rate in this study was thus minimum in the AS coating (0.83×10^{-4} mm^3 m^{-1}). This wear rate increased about 3 times in the FS coating, and about 7 times in the SF coating (Table 4).

Conclusion

The Ni-20%Cr coatings were successfully produced by spray and fuse, flame spray and arc-spray techniques. Microstructure, chemical composition and properties were strongly affected by the starting materials and spray processes. The densest and finest microstructure could be achieved by the arc-sprayed process. Chemical composition was rather similar in each coating but different from the starting materials due to an increase in oxide content caused by oxidation reaction occurring during spraying. In this study, the arc-sprayed Ni-20%Cr coating was the best candidate for further use in applications requiring long lifetime and wear tolerance because of its high adhesion strength, hardness and low wear rate.

Acknowledgements

The authors would like to thank the National Metals and Technology Center (MTEC) for financial support through the Thermal Spray Center, Chiang Mai University (TSC-CMU), the main thermal spray laboratory and Faculty of Science, Chiang Mai University for financial support. Thanks to Assist. Prof. Dr. Sittichai Wirojanupatump and Dr. Anucha Watcharapasorn for their fruitful discussion. ND would like to thank the Ministry of Education for financial support of her PhD program through Naresuan University, Thailand and Graduate School, Chiang Mai University.

References

Bhushan, B., and Gupta, B.K. 1997. Handbook of tribology: materials, coatings, and surface treatments, Krieger Publishing Company, Malabar, Florida.

Herman, H., and Sampath, S. 1996. Thermal spray coatings, in metallurgical and ceramic protective coatings, Ed. K.H. Stern, Chemical division, Naval Research Laboratory, Chapman & Hall, Washington DC, USA.

Pawlowski, L. 1995. The science and engineering of thermal spray coatings, John Wiley & Son, UK.

Sidhu, T.S., Prakash, S., and Agrawal, R.D. 2005. Characterization of NiCr wire coatings on Ni-

and Fe-based superalloys by the HVOF process. Surf. Coat. Technol.. Available online at www.sciendirect.com.

Smith, R.W., and Knigth, R. 1995. Thermal spraying 1: powder consolidation from coating to forming. J. Micro. 47(8): 32-39.

Sundararajan, T., Kuroda, S., Itagaki, T., and Abe, F. 2003. Stream oxidation resistance of HVOF thermal sprayed Ni-Cr coatings, Thermal spray 2003: Advancing the science & applying the technology, Ed. C. Moreau and B. Marple, ASM International, Ohio, USA.

Sundararajan, T., Kuroda, S., and Abe, F. 2005. Effect of thermal cycling on the adhesive strength of Ni-Cr coatings, Surf. Coat. Technol. 194: 290-299.

Thorpe, M.L. 1993. Thermal spray: Industry in transition. Adv. Mater. Process 143(5): 50-56.

Tucker, R.C., Jr. 1994. Thermal spray coatings, surface engineering, Vol.5, ASM Handbook, ASM International.